PCCP

Accepted Manuscript

This is an *Accepted Manuscript*, which has been through the Royal Society of Chemistry peer review process and has been accepted for publication.

Accepted Manuscripts are published online shortly after acceptance, before technical editing, formatting and proof reading. Using this free service, authors can make their results available to the community, in citable form, before we publish the edited article. We will replace this *Accepted Manuscript* with the edited and formatted *Advance Article* as soon as it is available.

You can find more information about *Accepted Manuscripts* in the **Information for Authors**.

Please note that technical editing may introduce minor changes to the text and/or graphics, which may alter content. The journal's standard **Terms & Conditions** and the **Ethical guidelines** still apply. In no event shall the Royal Society of Chemistry be held responsible for any errors or omissions in this *Accepted Manuscript* or any consequences arising from the use of any information it contains.

www.rsc.org/pccp

Ullmann Coupling Mediated Assembly of an Electrically Driven Altitudinal Molecular Rotor

Authors: Colin J. Murphy,[1] Zachary C. Smith,[1] Alex Pronschinski,[1] Emily A. Lewis,[1] Melissa L. Liranio,[1] Chloe Wong,[1] Christopher J. Ivimey,[1] Mitchell Duffy,[1,2] Wojciech Musial,[1,3] Andrew Therrien,[1] Samuel W. Thomas III,[1] E. Charles H. Sykes[1]*

1. *Department of Chemistry, Tufts University, Medford MA 02155*
2. *Current address: European Institute for Molecular Imaging, Westfälische Wilhelms Universität Münster, Germany*
3. *Current address: Center for Theoretical Physics, University of Berkeley, Berkeley, CA 94704.*

ABSTRACT

Surface-bound molecular rotation can occur with the rotational axis either perpendicular (azimuthal) or parallel (altitudinal) to the surface. The majority of molecular rotor studies involve azimuthal rotors, whereas very few altitudinal rotors have been reported. In this work, altitudinal rotors are formed by means of coupling aryl halides through a surface-mediated Ullmann coupling reaction, producing a reaction state-dependent altitudinal molecular rotor/stator. All steps in the reaction on a Cu(111) surface are visualized by low-temperature scanning tunneling microscopy. The intermediate stage of the coupling reaction is a metal-organic complex consisting of two aryl groups attached to a single copper atom with the aryl rings angled away from the surface. This conformation leads to nearly unhindered rotational motion of ethyl groups at the *para* positions of the aryl rings. Rotational events of the ethyl group are both induced and quantified by electron tunneling current versus time measurements and are only observed for the intermediate structure of the Ullmann coupling reaction, not the starting material or finished product in which the ethyl groups are static. We perform an extensive set of inelastic electron tunneling driven rotation experiments that reveal that torsional motion around the ethyl group is stimulated by tunneling electrons in a one-electron process with an excitation energy threshold of 45 meV. This chemically tunable system offers an ideal platform for examining many fundamental aspects of the dynamics of chemically tunable molecular rotor and motors.

KEYWORDS
Rotational dynamics, driven molecular rotors, low temperature STM, artificial molecular rotors

INTRODUCTION
Harnessing the motion of single molecules in a controlled manner is a vital step in the development of nanoscale devices such as fluid pumps, sensors, delay lines, and microwave signaling applications.[1–3] Attaining the next level of complexity in artificial molecular machines requires a deeper understanding of how to construct molecules that couple external energy to controlled mechanical motion. Of particular interest is the *electrical* excitation of molecular rotation as the small dimensions of today's electrical interconnects offer the greatest promise in terms of coupling external sources of energy to single

molecules. Studying the motion of molecules bound to surfaces also offers the advantage that a single layer can be assembled and monitored using the tools of surface science.[4–12] The majority of surface bound rotors discussed in the literature function as azimuthal rotors, with the axis of rotation perpendicular to the surface, while there are sparse examples of altitudinal surface-bound molecular rotors with the axis of rotation parallel to the surface.[11,13–15] Since the axes of rotation of azimuthal and altitudinal rotors are orthogonal, they will function differently in devices. An example is the molecular motors synthesized by Feringa and co-workers, which in one application function as azimuthal rotors that rotate near-macroscopic sized objects,[7] and in a second application function as altitudinal rotors and can transport a molecule across a surface.[11]

Using low-temperature scanning tunneling microscopy (LT-STM) we have previously examined the formation and surface diffusion of Ullmann coupling intermediates on Cu(111), where we tracked the reaction from reactants, through intermediates, to coupled biphenyl products.[16] The surface-bound phenyl groups that exist during the intermediate reaction stage on Cu(111) are tilted 30–45° off the surface plane (Figure 1) whereas the reactants and products should lie flat.[17,18] This ability to chemically form and investigate a stable surface bound intermediate inspired us to include a rotary functionality, an ethyl group, at the extremity of the molecular construct, that would allow us to study a very simple molecular rotor with atomic scale resolution. Controlling the extent of the Ullmann coupling reaction from reactants, through intermediates and then products allows us to examine the effect of proximity of the rotary group to the surface. This system bears resemblance to ethylbenzene in which the Csp^2 - Csp^3 bond rotation has been well studied by both experimental and theoretical methods.[19–21] A number of energetically preferred conformations of ethyl group relative to the phenyl ring have been established, the most stable having the ethyl chain positioned perpendicular to the benzene ring. A different local minima conformation, with the ethyl group parallel to the benzene, has been determined by IR and Raman spectroscopy.[19] The barrier of rotation around the Csp^2-Csp^3 bond from one global minima to the next is known to be around 45 meV[19,20,22]
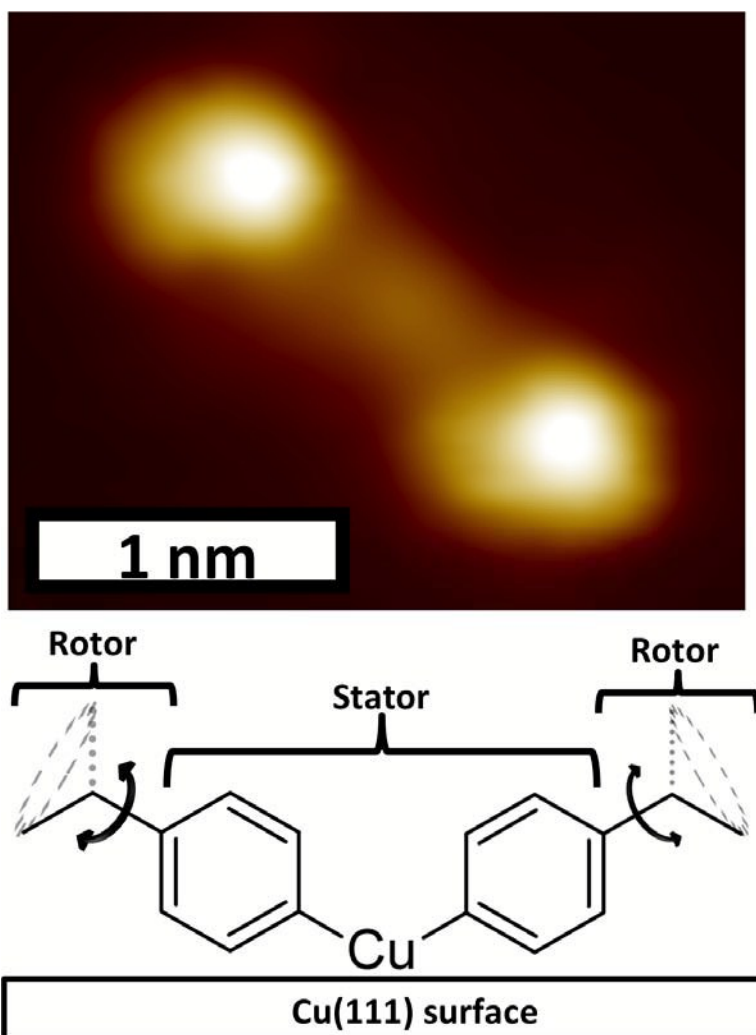
Figure 1: Upper panel: High resolution STM image of an Ullmann coupling intermediate in which the two pronounced lobes are the 4-ethylphenyl groups and the central feature is the Cu adatom linker that has been extracted from the Cu(111) surface (Scan condition: 20 mV 100 pA). Lower panel: Schematic of operation of the altitudinal rotor involving rotation of the ethyl groups.

The surface-catalyzed Ullmann coupling reaction offers a means to study the rotation of ethyl groups at the single molecule level. Time-resolved electron tunneling current measurements allow tracking of the rotation of the ethyl group around the Csp^2-Csp^3 bond. We report our quantitative measurement of the rotation of the ethyl group in the intermediate metal-organic complex of the surface-based Ullmann coupling reaction, but not in the starting material (1-bromo-4-ethylbenzene) or finished product (4,4'-diethylbiphenyl), indicating that steric hindrance with the surface blocks its rotation. We also examine the impact of steric hindrance from neighboring molecules on the ethyl group rotation. We demonstrate that tunneling electrons supplied by a LT-STM tip can electrically drive the rotation of this moiety, and that time-dependent measurements of the electron tunneling current can be used to extract information on the dynamics of this process.[23] Above an energy threshold of 45 meV, excitation is driven through a one-electron process and below that voltage; rotation occurs via a multi-electron process.

EXPERIMENTAL METHODS

The LT-STM instrument operates with a base pressure $< 10^{-11}$ mbar. 1-bromo-4-ethylbenzene and bromobenzene were acquired from Sigma Aldrich at 99.9 % purity and degassed by freeze/pump/thaw cycles. 1-bromo-4-ethylbenzene and/or bromobenzene were vapor deposited onto the Cu(111) sample held at 5 K through a precision leak valve. Low-temperature (<300 K) annealing treatments were performed in order to equilibrate the molecular ensembles and produce the intermediate structures by removing the sample from the cryogenically cooled stage of the microscope and placing it into a room-temperature sample holder in the ultra-high vacuum chamber for a predetermined length of time. Anneals above 300 K were achieved using a resistively heated manipulator arm. The samples were then cooled back to 5 K for high-resolution LT-STM imaging and I(t) measurements. The energy of the gas-phase ethylbenzene molecule was calculated at 10° increments of rotation of the ethyl substituent, using the Gaussian 09 software package with the B3LYP functional and the 6-311+G(d,p) basis set.[24]

RESULTS

We used low-temperature STM to track the progression of the surface-catalyzed Ullmann coupling reaction from weakly adsorbed reactants, through intermediates, to the biphenyl-based product. This enables us to characterize the relevant steps of the reaction with atomic-scale resolution as shown in Figure 2. Upon deposition onto the Cu(111) sample held at 5 K, 1-bromo-4-ethylbenzene adsorbs weakly and remains intact until 80 K (Figure 2 I). Annealing the sample to 220 K induces C–Br bond dissociation, and an intermediate structure is formed (Figure 2 II). We previously determined that these organometallic intermediates of the Ullmann coupling reaction consist of two aryl groups bound to a central Cu atom that has been extracted from step edges that separate terraces on the Cu(111) surface.[16] We never observed pits in the Cu terraces, which supported our conclusion that the Cu atoms incorporated in the organometallic intermediates originated from step edges.[16] These intermediates appear in STM images as linear tri-lobed structures with the central Cu atom appearing slightly less pronounced than the two external lobes, which represent the 4-ethylphenyl groups. Contrasting this di(4-ethylphenyl) cuprate intermediate (Figure 2 II) to the previously reported diphenyl cuprate intermediate (Figure 2 III), the external lobes are larger and the Cu atom is relatively less pronounced. Additionally, at scanning biases above ≈ 40 mV the lobes of the bis-(4-ethylphenyl) cuprate intermediate appear streaky in LT-STM images while no streaks are observed for the phenyl cuprate intermediate at higher biases. Such high frequency noise in STM images is a signature of atomic or molecular motion on a timescale of imaging which is typically ~ 1 min/frame. We therefore attribute the streakiness to motion of the ethyl group, which we quantify and compare to bare phenyl groups in detail below. Furthermore, this difference in how phenyl and 4-ethylphenyl groups appear in STM images allows us to identify the structure of the Ullmann cross-coupled intermediates formed from reaction of bromobenzene and 1-bromo-4-ethylbenzene. Further annealing the sample to 380 K completes the reaction producing the surface bound biaryl product, 4,4'-diethylbiphenyl which is seen mostly at step edges indicating that the Cu adatom in the complex is returned to the step edge as the product is formed (Figure 2 IV).[16]
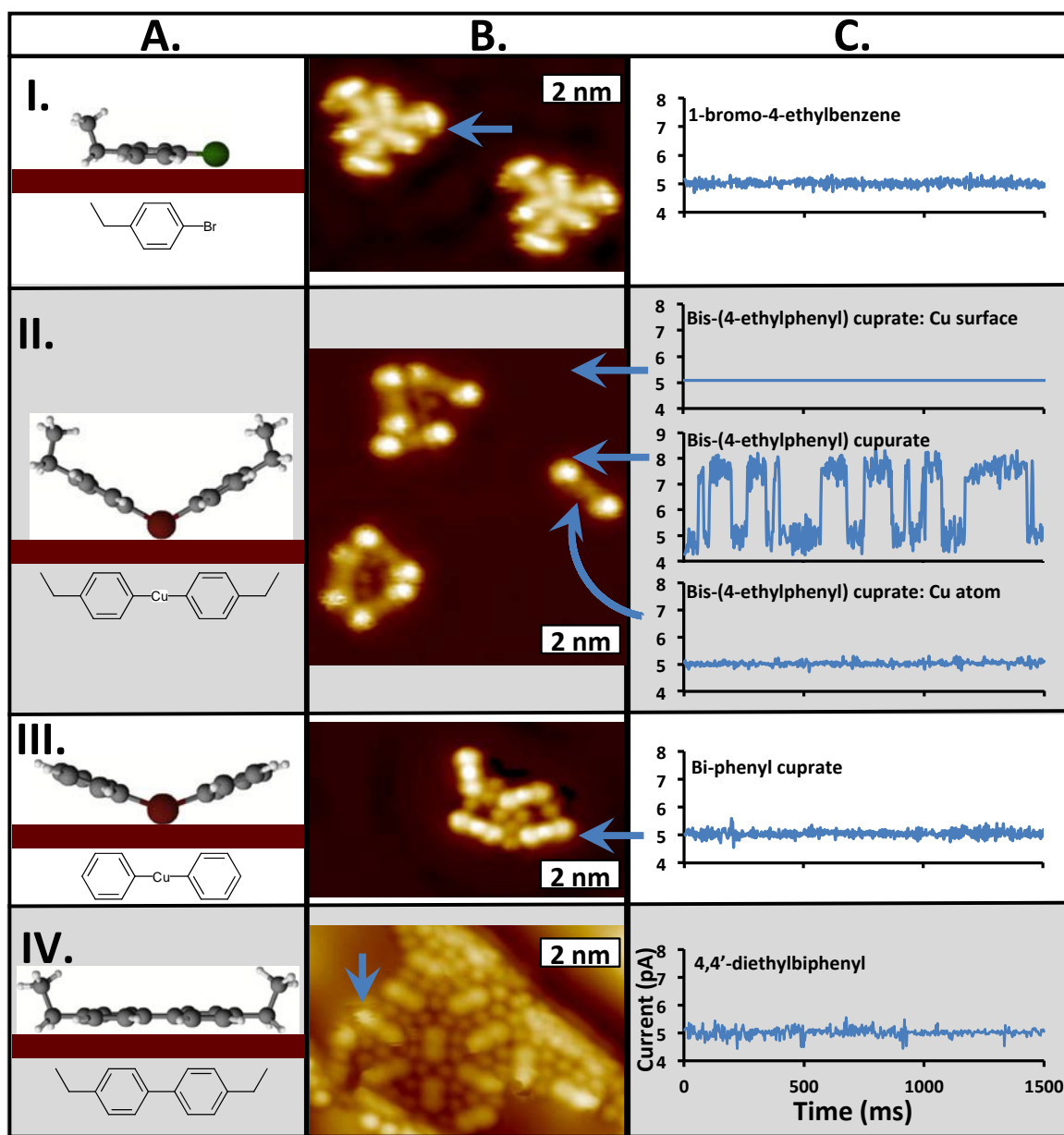
Figure 2: Column A shows side-view schematics and chemical structures of surface-bound the (I) 1-bromo-4-ethylbenzene reactant molecule (II) bis-(4-ethylphenyl) cuprate intermediate, (III) bi-phenyl cuprate intermediate, and (IV) 4,4'-diethylbiphenyl product molecule. Column B shows LT-STM images of the respective compounds on Cu(111). (Scan conditions: I. 30 mV, 50 pA; II. 50 mV, 50 pA; III. -150 mV, 50 pA; IV. 50 mV, 200 pA.) Column C shows representative tunneling current versus time (I(t)) measurements taken during the electron-induced excitation of the various species. Rotation is only apparent for the bis-(4-ethylphenyl) cuprate intermediate species at the extremes of the molecule where the ethyl groups reside. (Excitation conditions: 100 mV 5 pA)

We utilize a measurement mode of the LT-STM instrument called action spectroscopy, which can determine dynamic molecular conformational changes with sub-nanometer precision with a time resolution < 1 ms.[25] Briefly, the STM tip is placed asymmetrically to the side of the extremity of a mobile

group of a molecule, the feedback loop is turned off, a voltage is applied, and the resulting tunneling current is recorded as a function of time. The magnitude of the current depends on the distance separating the tip and the moving part of the molecule. Since the STM tip remains stationary, fluctuations in the tunneling current indicate changes in the orientation of the molecule or functional group being studied. Importantly, the alignment of the Ullmann coupling intermediate with respect to the underlying surface did not change during these experiments, indicating that azimuthal rotation of the whole organometallic intermediate around the axis of the Cu atom surface did not occur. Figure 2 shows current versus time (I(t)) traces alongside STM images of each of the chemical species. These traces are representative of those collected on multiple molecules. Figure 2 II displays a typical I(t) trace taken over the bare Cu surface and I(t) traces taken at different points of the molecule. The I(t) traces of both the starting material and finished product were always devoid of an step changes in the tunneling current that indicate molecular motion. To confirm that the changes in tunneling current observed in I(t) traces were due to the rotation of the ethyl group, we performed the same measurements at multiple points of the diphenyl-copper intermediate, which lacks the ethyl groups (Figure 2 III). No discrete changes appeared in the tunneling current traces in these experiments, which confirms that the I(t) signal arises from motion of the ethyl group. Data collected from the bis-(4-ethylphenyl) cuprate intermediate show two discrete tunneling current states. We determined a rate of rotational reorientation of the ethyl group by quantifying the number of transitions between these states. In terms of sterics, rotation was observed for the bis-(4-ethylphenyl) cuprate molecules isolated from each other on the surface or at the perimeter of a molecular island, however, molecules within the island interior did not usually display rotation under the listed excitation conditions, unless located next to a defect at the listed excitation conditions.

Next, to interrogate the mechanism of rotation of the ethyl group, action spectra across a range of sample biases were taken (Figure 3). A tunneling current of 1 pA for all collected data ensured that the rotation rates were well within the temporal detection threshold of the I(t) measurement.[26] Rotation was not observed for sample biases below ± 35 mV. At bias above ±45 mV, the rotation rate increased as the voltage increased, with a sharp upturn around ± 200 mV. The higher energy electrons excite vibrational modes of the molecule, which can relax through intramolecular vibration energy redistribution, exciting the lower energy ethyl rotation mode (typical ranges of energies of modes are shown in Figure 3 I).[27,28] The lower energy electrons may excite rotational modes directly or low-frequency bending modes that couple directly to the rotational mode. Evidence that tunneling electrons couple to rotational and vibrational modes as opposed to electronic excitation is the symmetry of the action spectra in Figures 2 and 5 about 0 V; vibrations and rotations are excited at the same energy regardless of the tunneling current direction, whereas the electronic states of metal surface bound molecules are not typically symmetric about the Fermi level. Although, the onset voltage of rotation at 45 mV is identical for both polarities, its rate is not. The electric field of the positively charged STM tip may interact with the intermediate in such a manner as to slow the rotation rate or the IET coupling efficiency may be lower for the negative voltage.
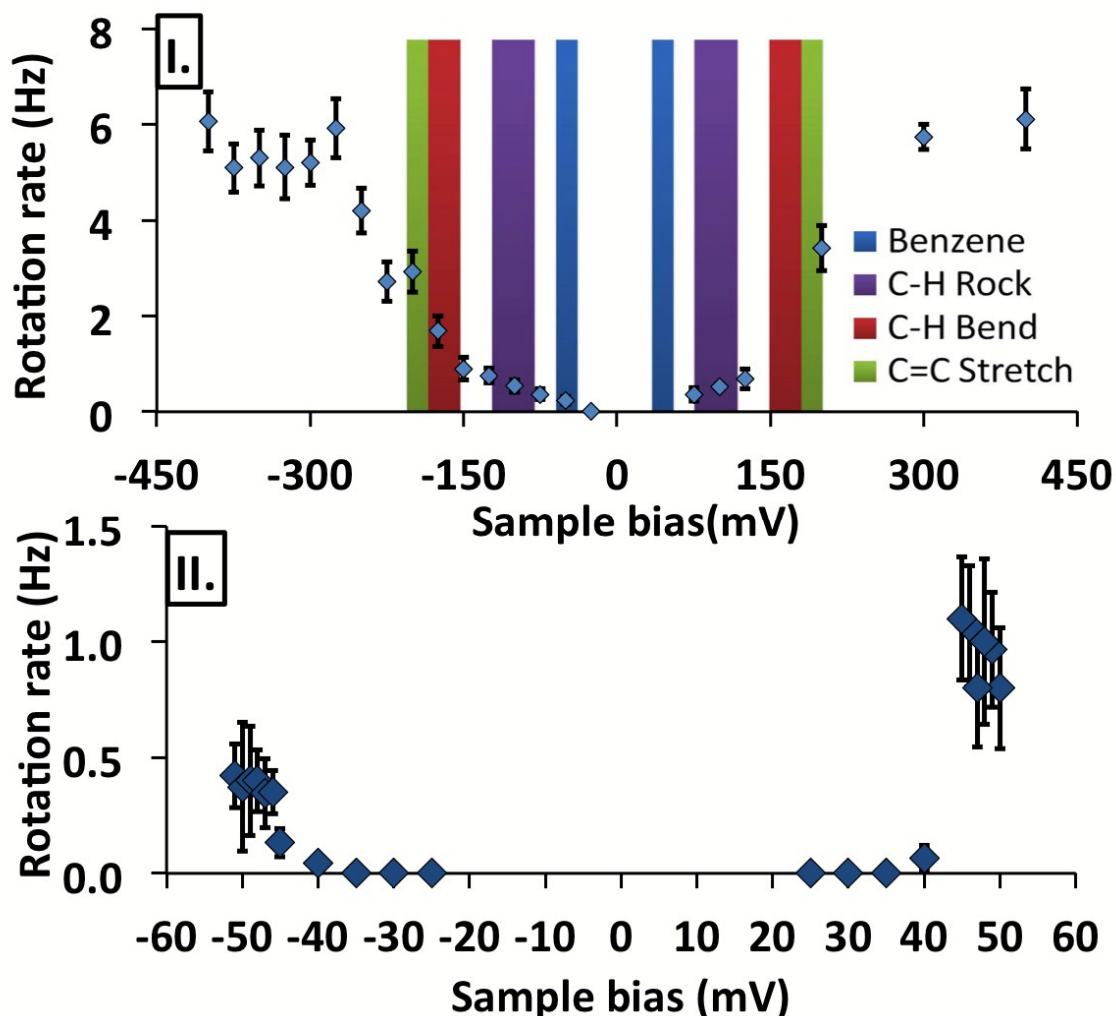
Figure 3: Action spectra for di(4-ethylphenyl) cuprate intermediate; plot of rotation rate vs. bias voltage (tunneling electron energy) with energies of representative vibrational modes highlighted. I. Data over a wide range of sample biases. II. Additional data focusing at lower bias voltages to show the onset of rotation at 45 meV. The error bars represent the 95% confidence interval for the rate parameter (i.e. the rate of rotational reorientations).

In order to understand our experimental action spectra, we performed theoretical calculations examining the rotation of the Csp^2-Csp^3 bond of a gas phase ethyl benzene molecule to determine the stable conformations of the ethyl group relative to the phenyl ring as well as the energetic barriers between then (Figure 4). Given the tilted geometry of the metal-organic intermediate in which the rotary ethyl tail is positioned at the furthest point from the surface this is a reasonable way to examine the energetics of rotation. Consistent with previous studies the most stable conformation has the ethyl chain orthogonal to the phenyl ring, and the barrier to rotation is ~45 meV.[19,20,22] Therefore, when the energy of the excited mode is higher than the rotational barrier E_{rot}, the rotational barrier can be overcome by excitation from a single inelastic-tunneling electron. However, when the energy of the incoming electrons, and therefore the highest energy vibrational mode, is less than E_{rot}, the rotation can only be induced by a multi-electron process.[29,30] For this so-called vibrational ladder climbing to occur the excited vibrational state lifetime must be comparable to the electron tunneling rate.[31,32] At 1 pA, the rate of electron tunneling is ~10^7

electrons/sec, which is low relative to typical vibrational state lifetimes on metals ($1\text{-}10\times10^{-12}$ sec); therefore, at low tunneling currents, above-threshold one-electron transitions dominate the rotational process.
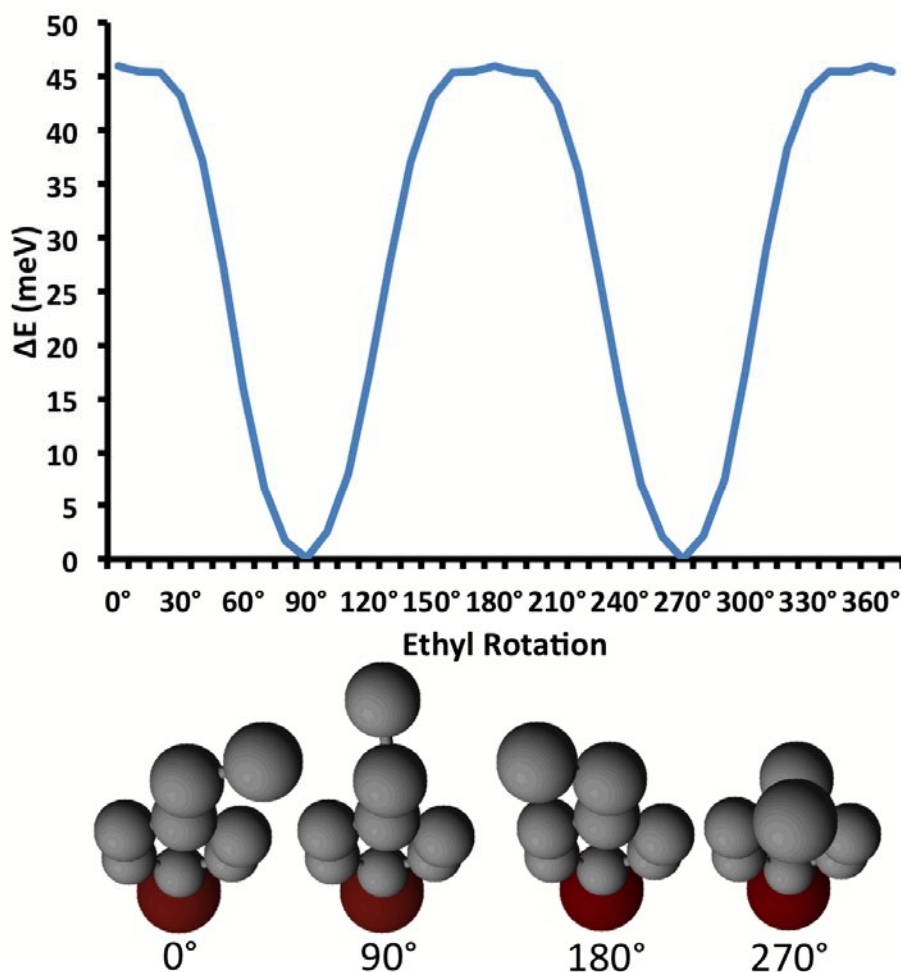
Figure 4: Rotational barrier around the $Csp^2\text{-}Csp^3$ bond of a gas-phase ethylbenzene molecule calculated using the B3LYP functional and the 6-311+G(d,p) basis set and schematics of conformations at dihedral angles of 0°, 90°, 180°, and 270°. Hydrogen atoms are omitted from the schematic for clarity.

In an inelastic tunneling electron induced process, the event rate, k, is proportional to the tunneling current, I, to the nth power, where n indicates the number of electrons that are involved in the process (Equation 1).

$$k \propto I^n \hspace{4cm} \text{Equation 1}$$

Figure 5A shows experimental data of rotation rate as a function of tunneling current for a series of applied biases. The data are fitted to the power-law, $\propto I^n$, and the slopes of the solid lines correspond to the electron order for a given voltage (i.e. electron energy). Figure 5B shows the electron order for a wide range of electron energies. The rotation of the system is a one-electron process above a threshold voltage

of 35 mV. Below this threshold value, only multi-electron processes can induce rotation of the ethyl groups, supporting the calculations and the experimentally measured rotational barrier of ~45 meV.[19,20] The switch from one- to multiple-electron rotational excitation mechanisms can also be visualized by plotting the rotation rate as a function of voltage at various tunneling currents (Figure 5C). It is apparent that for all energies at which excitation is a one-electron process, when five times more electrons are injected (i.e. 5 pA vs. 1 pA) the rotation rate increases by a factor of five.
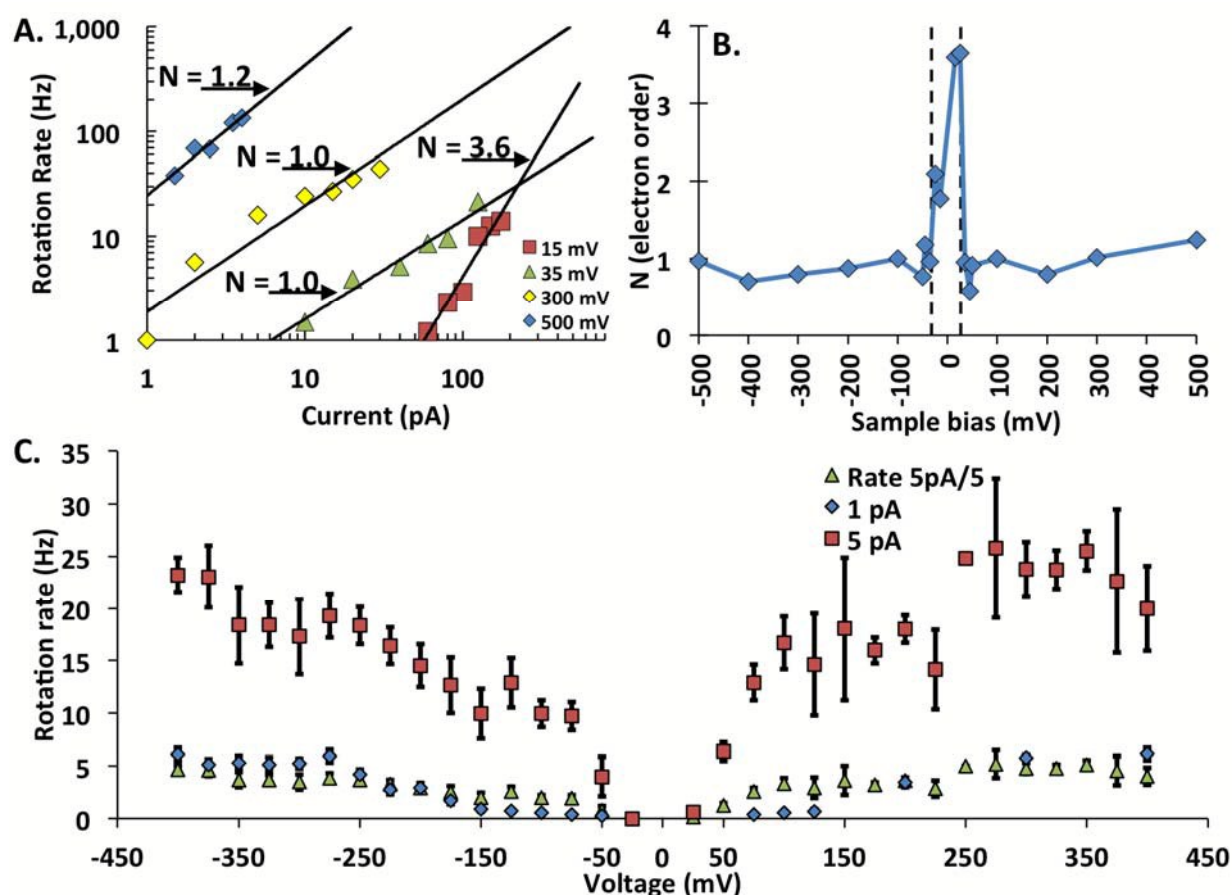
Figure 5: A) Rotation rate as a function of tunneling current for various applied biases (electron energies).The solid lines are power law fits to the data, the slope of the line, N, gives the electron order i.e. one vs. multiple electron induced rotation. B) A plot of electron order, N, as a function of sample bias voltage. The dashed lines denote the bias voltages below which N ≥ 2. C) Comparison of 5 pA and 1 pA excitation shows 1st order electron process over wide range of electron energies.

To further verify that we are measuring rotation motion of the ethyl group as opposed to the phenyl group we co-deposited bromobenzene and 1-bromo-4-ethylbenzene, and then annealed the surface to 220 K, forming a mixture of homo- and hetero-coupled intermediates. This allowed us to examine the difference between I(t) signatures of phenyl and 4-ethylphenyl groups with the same STM tip state (Figure 6). Similar to the homo-coupled sample STM images, the 4-ethylphenyl termini appear larger than the phenyl groups and appear streaky under perturbative imaging conditions, while the unalkylated phenyl groups do not appear streaky. I(t) traces taken over the 4-ethylphenyl vs. phenyl groups also show different characteristics, as was observed in the homo-coupled intermediate. These data further support that the

dynamical events are due to the ethyl functional group and not the motion of the phenyl unit. This opens up the interesting possibility to design altitudinal rotors by functionalizing the phenyl ring of the aryl halide at different positions with different alkyl groups or other substituents and then producing the Ullmann coupling intermediate on a surface where it can be studied in great detail. Additionally, since we have demonstrated that hetero cross-coupling occurs, rotors with two different termini that function differently can be imagined, perhaps one side functioning as a motor while the second side is a rotor, or with different barriers to rotation so that one side rotates at lower energy than the other.

Finally, to investigate the impact of steric hindrance by adjacent molecules on the ethyl group rotation rate, we examined clusters of the intermediate complexes in which the molecules were in close proximity. Figure 6 shows a collection of altitudinal rotors with varying proximity to other units that were electrically driven to rotate under identical excitation conditions (100 mV and 5 pA). From these measurements, it is apparent that the rotor that is spatially isolated from other units has the highest rotation rate. The rotors in closer proximity to other units have ~five times reduced rotation rates. This indicates that interactions between neighboring units are strong enough to hinder, but not totally block rotation as was seen for the flat-lying reactant and product molecules which displayed zero rotation rates. This behavior is distinct from both the surface-bound reactant bromoarene and product diethylbiphenyl for which interaction with the surface fully hinders the rotation of the ethyl group (Figure 2).
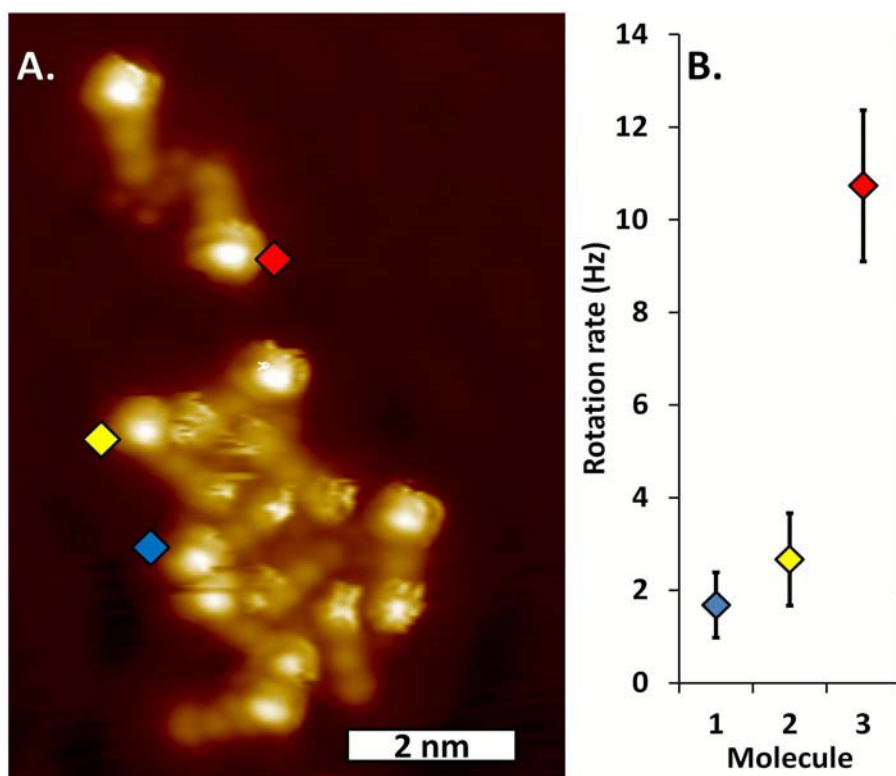
Figure 6: Impact of steric hindrance on ethyl group rotation. A) LT-STM image of a cluster of hetero- and homo-coupled organometallic intermediates formed from the reaction of bromobenzene and 1-bromo-4-ethylbenzene with the Cu(111) surface. B) Electrically induced rotational rate measurements taken at highlighted points. The red point represents the rotation of the unhindered molecule and the yellow and blue points progressively more hindered ethyl rotors. All data taken at identical electrical excitation conditions of 100 mV and 5 pA.

CONCLUSIONS

We have experimentally demonstrated a novel altitudinal surface-bound molecular rotor driven by inelastic electron excitation of molecular vibrations down to 45 meV. At energies lower than this threshold, multi-electron excitation of low-lying modes can couple to molecular rotation. The rotation of the ethyl group on a phenyl stator depends on the extent of the Ullman coupling reaction, for which rotation occurs in the intermediate organocopper complex but not in either the surface-bound reactants or products of the Ullmann reaction. The observation of ethyl group rotation for this organocopper intermediate indicates that rotation is dependent on the geometry of the molecule as phenyl groups on Cu, which we now understand are complexed with Cu adatoms, have been shown to tilt up from the plane of the surface.[17,18,33,34] We have demonstrated for the first time that in this tilted "V" shaped intermediate, ethyl groups in the *para* position relative to the C-Cu bond can rotate with a similar barrier to the gas phase molecule. When the ethyl groups are in close proximity to the Cu surface in both the starting material and finished product, however, the ethyl groups cannot be electrically driven to rotate. Neighboring molecules also affect the rotation rate of the intermediate rotor complex, which is promising feature in terms of future work involving coupled molecular rotors. Furthermore, the easy structural elaboration of this organometallic complex makes conceivable the introduction of chirality to produce a system capable of functioning as a molecular motor. Additionally, we envision rotary devices derived from unsymmetrically coupled complexes by varying the functional groups on each aromatic ring. Therefore, this chemically tunable molecular rotor platform offers a new well-defined model system with which to study a number of aspects of single molecule molecular rotors and motors.

AUTHOR INFOMATION

Corresponding Author

* E-mail: Charles.sykes@tufts.edu.

ACKNOWLEDGEMENTS

REFERENCES

1   G. S. Kottas, L. I. Clarke, D. Horinek and J. Michl, *Chem. Rev.*, 2005, **105**, 1281–1376.

2   X. Su and I. Aprahamian, *Chem. Soc. Rev.*, 2014, **43**, 1963.

3   X. Su, S. Voskian, R. P. Hughes and I. Aprahamian, *Angew. Chem. Int. Ed. Engl.*, 2013, **52**, 10734–10739.

4   J. Vacek and J. Michl, *Proc. Natl. Acad. Sci. U. S. A.*, 2001, **98**, 5481–6.

5   U. G. E. Perera, F. Ample, H. Kersell, Y. Zhang, G. Vives, J. Echeverria, M. Grisolia, G. Rapenne, C. Joachim and S.-W. Hla, *Nat. Nanotechnol.*, 2013, **8**, 46–51.

6   H. W. Kim, M. Han, H.-J. Shin, S. Lim, Y. Oh, K. Tamada, M. Hara, Y. Kim, M. Kawai and Y. Kuk, *Phys. Rev. Lett.*, 2011, **106**, 20–23.

7   R. Eelkema, M. M. Pollard, J. Vicario, N. Katsonis, B. S. Ramon, C. W. M. Bastiaansen, D. J. Broer and B. L. Feringa, *Nature*, 2006, **440**, 163.

8   B. Stipe, M. Rezaei and W. Ho, *Science*, 1998, **279**, 1907–1909.

9   Y. Shirai, A. J. Osgood, Y. Zhao, Y. Yao, L. Saudan, H. Yang, C. Yu-Hung, L. B. Alemany, T. Sasaki, J.-F. Morin, J. M. Guerrero, K. F. Kelly and J. M. Tour, *J. Am. Chem. Soc.*, 2006, **128**, 4854–4864.

10   B. Rodríguez-Molina, S. Pérez-Estrada and M. A. Garcia-Garibay, *J. Am. Chem. Soc.*, 2013, **135**, 10388–10395.

11   T. Kudernac, N. Ruangsupapichat, M. Parschau, B. Maciá, N. Katsonis, S. R. Harutyunyan, K.-H. Ernst and B. L. Feringa, *Nature*, 2011, **479**, 208–211.

12   M. Parschau, D. Passerone, K.-H. Rieder, H. J. Hug and K. Ernst, *Angew. Chem. Int. Ed. Engl.*, 2009, **48**, 4065–8.

13   D. Horinek and J. Michl, *Proc. Natl. Acad. Sci. U. S. A.*, 2005, **102**, 14175–14180.

14   X. Zheng, M. E. Mulcahy, D. Horinek, F. Galeotti, T. F. Magnera and J. Michl, *J. Am. Chem. Soc.*, 2004, **126**, 4540–4542.

15   G. London, G. T. Carroll, T. Fernández Landaluce, M. M. Pollard, P. Rudolf and B. L. Feringa, *Chem. Commun.*, 2009, 1712–1714.

16   E. A. Lewis, C. J. Murphy, M. L. Liriano and E. C. H. Sykes, *Chem. Commun.*, 2013, **50**, 0–2.

17   M. X. Yang, M. Xi, H. Yuan, B. E. Bent, P. Stevens and J. M. M. White, *Surf. Sci.*, 1995, **341**, 9–18.

18   M. Xi and B. E. Bent, *Surf. Sci.*, 1992, **278**, 19–32.

19   A. I. Fishman, A. E. Klimovitskii, A. I. Skvortsov and A. B. Remizov, *Spectrochim. Acta Part A Mol. Biomol. Spectrosc.*, 2004, **60**, 843–853.

20   Ö.¨Farkas, S. J. Salpietro, P. Császár and I. G. Csizmadia, *J. Mol. Struct. THEOCHEM*, 1996, **367**, 25–31.

21   J. Kříž and J. Jakeš, *J. Mol. Struct.*, 1972, 12, 367–372.

22   J. Klocker, A. Karpfen and P. Wolschann, *Chem. Phys. Lett.*, 2003, **367**, 566–575.

23   K. Motobayashi, S. Katano, Y. Kim and M. Kawai, *Bull. Chem. Soc. Jpn.*, 2013, **86**, 75–79.

24   M. J. Frisch, G. W. Trucks, H. B. Schlegel, G. E. Scuseria, M. A. Robb, J. R. Cheeseman, G. Scalmani, V. Barone, B. Mennucci, G. A. Petersson, H. Nakatsuji, M. Caricato, X. Li, H. P. Hratchian, A. F. Izmaylov, J. Bloino, G. Zheng, J. L. Sonnenberg, M. Hada, M. Ehara, K. Toyota, R. Fukuda, J. Hasegawa, M. Ishida, T. Nakajima, Y. Honda, O. Kitao, H. Nakai, T. Vreven, J. Montgomery, J. A., J. E. Peralta, F. Ogliaro, M. Bearpark, J. J. Heyd, E. Brothers, K. N. Kudin, V. N. Staroverov, R. Kobayashi, J. Normand, K. Raghavachari, A. Rendell, J. C. Burant, S. S. Iyengar, J. Tomasi, M. Cossi, N. Rega, J. M. Millam, M. Klene, J. E. Knox, J. B. Cross, V. Bakken, C. Adamo, J. Jaramillo, R. Gomperts, R. E. Stratmann, O. Yazyev, A. J. Austin, R. Cammi, C. Pomelli, J. W. Ochterski, R. L. Martin, K. Morokuma, V. G. Zakrzewski, G. A. Voth, P. Salvador, J. J. Dannenberg, S. Dapprich, A. D. Daniels, Ö. Farkas, J. B. Foresman, J. V. Ortiz, J. Cioslowski and D. J. Fox, *Gaussian, Inc., Wallingford CT,* 2009.

25   A. D. Jewell, H. L. Tierney, A. E. Baber, E. V. Iski, M. M. Laha and E. C. H. Sykes, *J. Phys.*

Condens. Matter, 2010, **22**, 264006.

26   Y. Kim, K. Motobayashi, T. Frederiksen, H. Ueba and M. Kawai, *Prog. Surf. Sci.*, 2015, **90**, 85–143.

27   H. Ueba, *Surf. Sci.*, 2007, **601**, 5212–5219.

28   H. L. Tierney, A. E. Baber, A. D. Jewell, E. V. Iski, M. B. Boucher and E. C. H. Sykes, *Chem. Eur. J.*, 2009, **15**, 9678–9680.

29   H. Ueba, T. Mii, N. Lorente and B. N. J. Persson, *J. Chem. Phys.*, 2005, **123**, 084707.

30   G. P. Salam, M. Persson and R. E. Palmer, *Phys. Rev. B*, 1994, **49**, 10655–10662.

31   R. Walkup, D. Newns and P. Avouris, *Phys. Rev. B*, 1993, **48**, 1858–1861.

32   S. G. Tikhodeev and H. Ueba, *Phys. Rev. B*, 2004, **70**, 8.

33   M.-T. Nguyen, C. A. Pignedoli and D. Passerone, *Phys. Chem. Chem. Phys.*, 2011, **13**, 154–60.

34   D. Jiang, B. G. Sumpter and S. Dai, *J. Am. Chem. Soc.*, 2006, **128**, 6030–1.